

SUPPLEMENTARY INFORMATION

Molecular mimicry between Anoctamin 2 and Epstein-Barr virus nuclear antigen 1 associates with multiple sclerosis risk

Katarina Tengvall^{1,2}, Jesse Huang^{1,2}, Cecilia Hellström³, Patrick Kammer⁴, Martin Biström⁵, Burcu Ayoglu⁶, Izaura Lima Bomfim^{1,2}, Pernilla Stridh^{1,2}, Julia Butt⁴, Nicole Brenner⁴, Angelika Michel⁴, Karin Lundberg^{2,7}, Leonid Padyukov^{2,7}, Ingrid E. Lundberg^{2,7}, Elisabet Svenungsson⁷, Ingemar Ernberg⁸, Sigurgeir Olafsson⁹, Alexander Dilthey^{10,11}, Jan Hillert¹, Lars Alfredsson^{12,13}, Peter Sundström⁵, Peter Nilsson^{3*}, Tim Waterboer^{4*}, Tomas Olsson^{1,2*}, Ingrid Kockum^{1,2*}.

*shared author

¹ Neuroimmunology Unit, The Karolinska Neuroimmunology & Multiple Sclerosis Centre, Department of Clinical Neuroscience, Karolinska Institute, Stockholm, Sweden

² Centrum for Molecular Medicine, Karolinska University Hospital, Stockholm, Sweden

³ Division of Affinity Proteomics, Department of Protein Science, KTH Royal Institute of Technology & SciLifeLab, Stockholm, Sweden

⁴ Infections and Cancer Epidemiology, Infection, Inflammation and Cancer Research Program, German Cancer Research Center (DKFZ), Heidelberg, Germany

⁵ Department of Pharmacology and Clinical Neuroscience, Umeå University, Umeå, Sweden

⁶ Division of Cellular and Clinical Proteomics, Department of Protein Sciences, KTH Royal Institute of Technology & SciLifeLab, Stockholm, Sweden

⁷ Division of Rheumatology, Department of Medicine Solna, Karolinska Institutet, Stockholm, Sweden

⁸ Department of Microbiology, Tumor and Cell Biology, Karolinska Institute, Stockholm, Sweden

⁹ deCODE genetics/Amgen, Reykjavik, Iceland.

¹⁰ Wellcome Trust Centre for Human Genetics, University of Oxford, Oxford, United Kingdom.

¹¹ Institute of Medical Microbiology and Hospital Hygiene, Heinrich-Heine-University Düsseldorf, Germany

¹² Institute of Environmental Medicine, Karolinska Institute, Stockholm, Sweden;

¹³ Centre for Occupational and Environmental Medicine, Stockholm County Council, Stockholm, Sweden

Abbreviations

aa amino acid/s; **ANO2** Anoctamin 2; **AP** attributable proportion; **CAC** continuous association curve; **CIS** clinically isolated syndrome; **CNS** central nervous system; **CSF** Cerebrospinal fluid; **EBNA1** Epstein-Barr virus nuclear antigen 1; **EBV** Epstein-Barr virus; **GWAS** genome wide association study; **HLA** human leukocyte antigen; **IgG** immunoglobulin G; **IM** infectious mononucleosis; **IIM** idiopathic inflammatory myopathy; **LD** linkage disequilibrium; **MADs** median absolute deviations; **MFI** median fluorescence intensity; **MHC** major histocompatibility complex; **MS** multiple sclerosis; **OR** odds ratio; **PC** principal component; **RA** rheumatoid arthritis; **SLE** systemic lupus erythematosus; **SNP** single nucleotide polymorphism; **95%CI** ninety-five percent confidence interval

TABLE OF CONTENTS

ABBREVIATIONS	2
MATERIAL S1. GENOTYPING QUALITY CONTROL AND ANALYSES	3
<i>Genome-wide association analyses</i>	3
<i>HLA genotyping and association analyses</i>	4
MATERIAL S2. DESCRIPTION OF COHORTS	4
MATERIAL S3. DESCRIPTION OF SEROLOGICAL MEASUREMENTS.....	5
MATERIAL S4. DESCRIPTION FOR ANO2 AND EBNA1 CROSS REACTIVITY	6
<i>ANO2 autoantibody epitope mapping</i>	6
<i>Sequence alignment of ANO2 and EBNA1</i>	6
<i>Pilot experiments for cross reactivity</i>	6
<i>Follow-up experiments for cross reactivity in a larger sample set</i>	7
MATERIAL S5. BATCH CORRECTION AND THRESHOLD DEFINITIONS	7
MATERIAL S6: STATISTICAL ANALYSES.....	8
FIGURE S1. ANO2 EPITOPE MAPPING AND PROTEIN FRAGMENT COMPETITION.	10
FIGURE S2. GENOME-WIDE ASSOCIATION ANALYSES OF ANTI-ANO2 ANTIBODY LEVELS.....	11
FIGURE S3. CORRELATION OF ANTI-ANO2 INTENSITY VALUES BETWEEN ASSAYS AND REPRESENTATIONS.	12
FIGURE S4. MULTIDIMENSIONAL SCALING PLOTS USING ANCESTRY INFORMATIVE MARKERS	13
FIGURE S5. HIGH CORRELATION BETWEEN ANO2 ANTIBODY REACTIVITY IN CEREBROSPINAL FLUID AND PLASMA.	14
FIGURE S6. CORRELATION BETWEEN ANO2 AND EBNA1 ANTIBODY REACTIVITY IN CEREBROSPINAL FLUID AND PLASMA.	15
TABLE S1. ASSOCIATION OF ANTI-ANO2 ANTIBODY LEVELS WITH DISEASE.	16
TABLE S2. ANO2 SEROPOSITIVITY ASSOCIATION WITH MULTIPLE SCLEROSIS AT DIFFERENT CUTOFFS.	17
TABLE S3. ODDS RATIOS FOR MULTIPLE SCLEROSIS WITH DIFFERENT COMBINATIONS OF THE RISK FACTORS	18
TABLE S4. TOP SNPs ($p < 10^{-4}$) FROM GWAS USING THE OMNIEXPRESS CHIP	19
TABLE S5. HLA ALLELES ASSOCIATED WITH ANTI-ANO2 ANTIBODY LEVELS	25
TABLE S6. ANO2 [AA 1-365] AUTOANTIBODY REACTIVITY ASSOCIATION WITH DISEASE.	26
TABLE S7. DEMOGRAPHIC DATA OF THE INITIAL, VALIDATION, AND WHOLE COHORTS.	27
REFERENCES.....	28

Material S1. Genotyping quality control and analyses

Genotyping was carried out at deCODE (1) using Illumina OmniExpress chip with 716 503 SNPs mapped to the Human Assembly Feb.2009 (GRCh37/hg19). We excluded SNPs with less than 2% frequency in the population, less than 98% genotyping rate and SNPs that were not in Hardy-Weinberg equilibrium ($p < 0.0001$). After quality control, 615 763 SNPs (86%) remained.

From 13781 genotyped individuals, the following were excluded; 1 individual with more than 2% missing genotypes, 71 individuals with high heterozygosity rates (> 0.032), 127 individuals with discordant sex information, 344 individuals who were ancestral outliers ($Z = 6$ SD), and 311 individuals were closely related (IBD π -hat 0.175). This left 12 778 individuals (6 983 multiple sclerosis (MS) cases, 5 795 controls) remaining that passed quality control. Out of these, we also had serological data for 11 936 individuals, which was used in the genome wide association study (GWAS).

Genotypes from 331 537 SNPs were available from another genotyping array, the MS replication chip, through collaboration with the International Multiple Sclerosis Genetics Consortium (IMSGC). The MS replication chip is a custom content array that includes rare variants ($< 2\%$ MAF) that we excluded from this analysis (2), and 94 598 SNPs remained after quality control (MAF $> 2\%$, $< 98\%$ genotyping success rate, and HWE $p < 0.0001$). From 16381 (4210 males, 12 132 females, 39 ambiguous) genotyped individuals, the following were excluded; 27 individuals with high heterozygosity rates (> 0.0769), 309 individuals with discordant sex information, 637 individuals were population outliers ($Z = 6$ SD), and 461 individuals were closely related (IBD π -hat 0.175). In total, 13160 individuals also had serology data and were included in subsequent analyses. In GWAS using OmniExpress SNPs when adjusting for HLA-alleles, *i.e.* using HLA alleles imputed from the MS replication chip, the number of individuals was 11 069.

Genome-wide association analyses

Genome wide association analyses of anti-ANO2 antibody levels was performed in individuals from the Whole cohort, which was previously genotyped both at deCODE Genetics (1) using Illumina OmniExpress chip and through a collaboration with the International MS Genetics Consortium (IMSGC) using the MS replication chip. Ancestrally informative markers (AIM) were included on the MS replication chip to enable estimates of population stratification ($n = 3 736$). Of these, 2 307 AIM were also available from the OmniExpress chip, and used in the quality control. Based on the selected AIM markers, a relationship matrix was generated and plotted as multi-dimensional scaling plot showing that the visualized population substructure was explained by self-reported origin of the subjects and not by ANO2-seropositivity, MS-status, or study cohort (**Fig. S3**). MS-status, age, sex, EBNA1-serostatus, study type, and principal components (PCs) to correct for population stratification, were included as fixed covariates in all GWAS's. PCs 1-5 (OmniExpress) and PCs 1-6 (MS replication chip) were calculated using Smart-PCA (3).

Genome-wide association data analyses were performed with PLINK v. 1.90 (4) and in R v. 3.3.3 with R-studio (v. 1.1.442) using the R-package GenABEL v. 1.8-0 (5) and hglm v. 1.0-0

(6). The R-package *cgmisc* v. 2.0 (7) was used for visualization and defining SNPs in linkage disequilibrium (LD) where the threshold for LD was set at $r^2 > 0.6$. Genome-wide significance threshold was set at the generally accepted level of $P = 5 \times 10^{-8}$ (8).

HLA genotyping and association analyses

Genotypes from the MS replication chip (2, 9) after quality control of SNPs and individuals were used for imputation of HLA allele variants for MHC class I and II using the software *HLA*IMP:02* (10) and an extended reference panel (including a Swedish cohort for HLA class II). After removal of population outliers, 282 HLA alleles, spread over 11 loci, were available for 7 062 MS cases and 6 098 controls with serology data. We tested each HLA allele in turn for association with anti-EBNA1 and log₁₀ transformed anti-ANO2 antibody levels using logistic regression where carrier status was treated as a binary variable. The HLA allele association analyses were corrected for MS, sex, age, study type, EBNA1-status (except in the EBNA1-association analysis), and six PCs (from MS replication chip data). The same alleles were the most associated ones without adjusting for EBNA1-status as well as when the analysis was rerun in 11 805 individuals excluding persons with imputation quality score below 0.7 at either allele in the DRB1 locus. The reason for not removing individuals with bad quality alleles before the association analysis was to avoid bias favoring high frequency alleles over low frequency alleles, which generally have a lower quality score. For the RA sample cohort HLA alleles were imputed using *SNPtoHLA* (11) and available for 1 214 individuals.

Material S2. Description of cohorts

Plasma samples were included from case-control cohorts consisting of 8 746 MS cases and 7 228 controls (after removal of missing data, i.e., individuals lacking phenotype information or sample measurement, **Table S7**). They were recruited from three Swedish nation-wide epidemiological studies and one clinical based study: EIMS (12), GEMS (13), IMSE (14), and STOP-MS (15). All patients were examined and diagnosed by a neurologist and fulfilled the McDonald criteria (16, 17). The patients recruited to the EIMS and STOP-MS study cohorts were incident cases whereas those in GEMS and IMSE were prevalence-based. Differences in, e.g., disease duration, age at sampling, and disease severity, were considered in the analyses by adjusting for study type (*i.e.* incidence versus prevalence) and age at sampling (in years). Controls were randomly selected from a national population registry and matched with patients in the EIMS and GEMS studies by residential area, sex, and age (within predetermined 5-year age groups). Controls were not available from IMSE or STOP-MS. The study subjects also had records of self-reported birth country (Sweden, other Scandinavian countries, Finland, other, or unknown) for both the subjects and their parents where the record of country ethnically furthest away from Sweden was the one used. In the analysis in this study patients and controls were divided into the following three sample sets for the analyses: **Whole cohort**, including all individuals; **Initial cohort**, the same individuals as our previous study (18); and **Validation cohort**, a replication sample set with all individuals except those included in our previous work (18, 19).

In additional, a **Pre-MS cohort** consisting of a prospective case-control study on biobank samples drawn before symptom onset was included. Swedish multiple sclerosis registry

containing 11 196 MS cases (February 2012) was cross-linked with three Swedish microbiological biobanks containing the remainders of sera (stored at -20°C) after clinical microbiological analyses performed at the University Hospitals of Skåne and Gothenburg, and the Public Health Agency of Sweden. Median and mean age at sampling was 25 years (range 2-39). Individuals who did not develop MS served as controls and were matched to cases by biobank, sex, date of sampling, and date of birth. The final number of matched sets of cases and controls were 474 and the mean difference in age at sampling was 65 days and six days for date of serum collection between cases and controls. For six individuals there were no matching case or control due to dropout of study participants after the matching process, but these individuals were still included in the analyses. In total, 478 MS cases and 476 controls were included in the analyses of the Pre-MS cohort.

Sample sets of other inflammatory diseases consisted of: an RA cohort, 986 newly diagnosed rheumatoid arthritis (RA) patients and 689 controls, from the Swedish population-based RA case-control study EIRA (20); an IIM cohort, 219 patients with idiopathic inflammatory myopathy (IIM) (21); and an SLE cohort, 349 patients with systemic lupus erythematosus (SLE) and 306 age and sex matched population controls (22). The SLE-matched controls were also used in the analyses of the IIM cohort.

Material S3. Description of serological measurements

Pseudonymized plasma samples (Initial, Validation, Whole, Pre-MS and RA cohorts) were shipped on dry ice to the German Cancer Research Center (DKFZ; Heidelberg, Germany) for analysis by lab personnel, blinded to sample origin and case-control status, using Multiplex Serology, a fluorescent bead-based glutathione S-transferase (GST) capture immunoassay, as described previously (23). Briefly, SeroMap beads (Luminex, Austin, TX, USA) were covalently derivatized with glutathione-casein (GC). Antigens were bacterially expressed as GST-fusion proteins and in-situ affinity purified directly on GC-coupled bead sets (24). Antigen-loaded beads were mixed and simultaneously presented to plasma samples (final plasma dilution 1:1 000). Bound primary antibodies were detected using a biotinylated anti-human IgG secondary antibody (#109-065-064, Jackson ImmunoResearch, West Grove, USA). IgG antibody reactivities against ANO2-derived fragments ANO2 [aa 79-167] and ANO2-long [aa 1-365], and EBV-derived EBNA1 [aa 385-420] were determined. Incubation with streptavidin-R-phycoerythrin (Strep-PE) enabled detection and quantification of antibody reactivities on Luminex® 100/ 200 analyzers (Luminex Corp., Austin, TX, USA). Sero-reactivity against the tested antigens was expressed as the median fluorescence intensity (MFI) of at least 100 bead counts per bead set and plasma sample. The batch corrected MFI values (see details in **Material S5**) are henceforth referred to as signal intensities.

Antibody measurements in the plasma samples from the IIM and SLE cohorts were performed at SciLifeLab (Stockholm, Sweden). The samples were analyzed in three batches; the samples from patients with IIM in one, and the samples from patients with SLE and population controls age and sex matched to the SLE samples equally distributed in two. The analyses were performed as

the bead-based antigen array previously described (18), with some minor alterations. In short, a total of 358 antigens, including an ANO2 protein fragment (Human Protein Atlas) and full length EBNA1 (Abcam ab138345), were covalently coupled to color-coded magnetic beads (MagPlex, Luminex Corp., Austin, TX), and subsequently incubated with samples diluted 1:250. The MFI from R-phycoerythrin-conjugated Fc γ -specific goat anti-human IgG F(ab')₂ fragment (H10104, Invitrogen) bound to captured human IgGs was acquired using a FlexMap3D instrument (Luminex Corp., Austin, TX, USA). The sample specific background adjusted MFI values for the IIM and SLE cohorts (see details in **Material S5**) are henceforth referred to as signal intensities.

Material S4. Description for ANO2 and EBNA1 cross reactivity

ANO2 autoantibody epitope mapping

Epitope mapping of ANO2 was performed to fine-tune previous work (18) by using 15 N-terminally biotinylated 15-mer peptides with 14 amino-acids overlap covering region [aa 128-156]. A set overlapping with the samples used for epitope mapping previously (18) (196 MS cases and 185 controls from the Initial cohort) as well as an additional sample set (189 MS cases and 195 controls from the Initial cohort) were analyzed. The assay was performed as previously described (18) with the addition of a fixating step using 0.2% paraformaldehyde, before incubation with the detection antibody (Invitrogen H10104).

Sequence alignment of ANO2 and EBNA1

Basic Local Alignment Search Tool (BLAST; <https://blast.ncbi.nlm.nih.gov/Blast.cgi>) was used for detection of similarities between the ANO2 and EBNA1 full-length protein sequences, to investigate possible regions of cross-reactivity.

Pilot experiments for cross reactivity

Initial competition assays between various EBNA1 and ANO2 representations and the corresponding antibodies were performed at SciLifeLab (Stockholm, Sweden) to test for cross reactivity. Two bead arrays were prepared according to previously described protocol (18). The first array consisted of in-house protein fragments representing ANO2 (Human Protein Atlas, HPRR3070036 [aa 79-167]) and 36 other proteins (Human Protein Atlas, 35 fragments, 27-145 aa in length), selected based on previously generated data (18). The second array consisted of ten N-terminally biotinylated peptides (Sigma-Aldrich PEPscreen) representing EBNA1 [aa 69-88, 101-120, 122-141, 385-404, 391-410, 393-412, 401-420, 421-440, 425-444, 431-450, 436-455] (**Fig. 2B**) and two representing ANO2 [aa 128-142, 135-149] (**Fig. S1A**) defined as non-reactive and reactive, respectively, in the described ANO2 autoantibody epitope mapping (**Fig. S1B**).

Seven plasma samples from MS patients, ranging between high and low anti-ANO2 and anti-EBNA1 signal intensities in our previous screening (18), were diluted 1:150 in assay buffer adapted to the protein fragment assay (0.05% PBS-Tween20, 3% BSA, 5% low-fat milk, and 160 μ g/ml His₆ABP) and the peptide assay (0.05% PBS-Tween20, 3% BSA, and 10 μ g/ml

Neutravidin). Each sample was split into aliquots and individually blocked with different representations of EBNA1 and ANO2. In the first assay, four protein fragment representations of EBNA1 (Abcam ab138345 [aa 1-641], Abcam ab68991 [aa 1-90, 408-498], ProSpec ebv-276 [aa 408-641], and Nordic BioSite PPT-53340 [aa 1-90,408-498]) and the reactive in-house ANO2 fragment [aa 79-167] were used as blocking fragments at 1 μ M. In the second assay all 12 peptides included in the bead array were used as blocking fragments at 30 μ M. Additionally, two wells per sample (duplicates) without blocking fragments were included per plate and assay. All diluted samples incubated for 1 hour at room temperature with slight shaking (80rpm) to allow potential competition before incubation with the respective bead arrays. The rest of the assays were performed as previously described (18), with the addition of a fixating step using 0.2% paraformaldehyde, before incubation with the detection antibody (Invitrogen H10104).

In each assay, the fold change was calculated by dividing the mean of the signal intensities obtained from the duplicates without blocking, by the respective signal intensities obtained with blocking. The mean fold change per analyte and blocking reagent was subsequently calculated across all seven samples and visualized as heatmaps (**Fig. 2B** and **Fig. S1D**). Wilcoxon rank-sum test was used for each peptide to test effect differences of the blocking fragments.

Follow-up experiments for cross reactivity in a larger sample set

Based on the pilot experiments in a small sample set ($n = 7$) and 11 peptide representations of EBNA1, one peptide for ANO2 [aa 135-149] and two peptides for EBNA1 [aa 401-420] and [aa 425-444] were selected to evaluate the cross-reactivity in a larger sample set. In total, samples from 82 MS cases were selected from the Whole cohort based on the data presented here to represent both high and low anti-ANO2 and anti-EBNA1 antibody levels (including all combinations). The peptides were coupled to beads as previously described (18). The samples were diluted 1:150 in assay buffer (0.05% PBS-Tween20, 3% BSA, and 10 μ g/ml Neutravidin) and subsequently split into four equal aliquots. Each aliquot was blocked with either one of the peptides at 30 μ M or equivalent volume of 0.05% PBS-Tween20. All diluted samples were incubated for 1 hour at room temperature with slight shaking (80rpm) to allow potential competition before incubation with the bead array. The rest of the assay was performed as in the pilot experiment, following the addition of blocking reagents.

Material S5. Batch correction and threshold definitions

Serological measurements for Initial, Validation, Whole, Pre-MS, and RA cohorts were conducted in several batches. To reduce batch effects, two plates of inter batch controls ($n \sim 180$ samples) were analyzed within each batch and used to correct variation to a single reference. Control measures were modeled using either a non-linear model (e.g., logarithmic, exponential, etc.) or standard linear model. The signal intensities presented are batch-corrected. The cutoff for ANO2-seropositivity was determined at the signal intensity of 420. Since, anti-ANO2 antibody levels were significantly increased in MS cases compared to controls and the exact cutoff for ANO2-seropositivity is not given, we set out to define at what signal intensity the maximum change in association with MS occurs (continuous association curve, CAC). In summary, a continuous association curve was created by analyzing a series of overlapping “moving” strata defined by fixed percentile ranges of anti-ANO2 signal intensity. Each ANO2 stratum (“moving”) was then analyzed in association with MS incidence in comparison to the lowest

stratum (“reference”). The association estimates by anti-ANO2 signal intensity were then plotted and modeled to determine the inflection point (i.e. point of maximum change in association with MS), which was used as a cutoff to approximate the point of biological effect. For comparison, the more generally used cutoff approaches: median plus one up to 15 standard deviations (SD) in controls, mean in controls, and quantiles cutoff (top 25% versus bottom 25% with the grey zone removed), are presented in **Table S2**.

Antibody levels against EBNA1 [aa 385-420] were dichotomized into high (EBNA1-high) and low (EBNA1-low) antibody reactivity to define an individual’s EBNA1-status as has been done previously (25). The signal intensity cutoff of 5 490 (median in controls from Whole cohort) was used in analyses of Initial, Validation, and Whole cohorts. In the Pre-MS cohort and RA-cohort, EBNA1-status was defined by the median signal intensity in controls of each dataset (4 397 and at 3 912, respectively). To define individuals who were not infected by the virus, i.e., EBNA1-seronegative, the cutoff was set at an anti-EBNA1 signal intensity below 200.

The data from the IIM and SLE cohorts was background adjusted per sample by transforming the signal intensities into the number of median absolute deviations (MADs) from the sample median, based on the signal intensities from in total 358 antigens and adjusted with +6 MADs (lowest value in the complete dataset plus one) for all intensities to avoid negative values in log₁₀ transformation. The samples were dichotomized into low and high anti-EBNA1 antibody levels based on the median among controls (MADs = 1 237).

Material S6: Statistical analyses

Statistical analyses were performed using R (26). The nonparametric Wilcoxon rank-sum test was applied for statistical analysis of differences for two-group comparisons. Fisher’s exact test was used for the statistical evaluation of frequency or categorical data. Spearman’s rank correlation test (rho; a nonparametric measure of rank correlation) and Pearson’s product-moment correlation was used for defining correlation between values. Analyses were performed in the Whole cohort using continuous values of anti-ANO2 signal intensity normalized with a log₁₀ transformation, if nothing else is specified. Additive interactions were determined by the attributable proportion (AP) due to interaction, using logistic regression and 95% confidence intervals (CI), in R by utilizing published scripts (27). In the linear and logistic regression models, the analyses were adjusted for MS-status, sex, age, EBNA1-status (except when testing for association with EBNA1), and study type (incident or prevalence cases).

Figure S1. ANO2 epitope mapping and protein fragment competition. Alignment of EBNA1 fragments and peptides to full-length EBNA1 (A) and of ANO2 15-mer peptides and protein fragments to full length ANO2 (B). ANO2 epitope mapping was performed in two separate sample sets of both MS cases and controls from the Initial cohort, one overlapping with the sample set used in previously (18) and one additional sample set, using the 15-mer peptides (**Material S4**). Signal intensities from the epitope mapping were background adjusted by subtracting the signal intensity from the neutravidin coated negative control bead, and subsequently visualized as line plots (C). The amino acid sequence in common between most reactive peptides was considered as the reactive epitope. ANO2 [aa 135-149] (pink) was the peptide with highest overall reactivity across the datasets and therefore chosen to represent the reactive epitope of ANO2 in the competition assays (**Fig. 2B and 3**). ANO2 [aa 128-142] consistently showed a complete lack of reactivity and was therefore chosen as the corresponding negative control (**Fig. 2B**). The median fold change between blocking and not blocking with protein fragments, representing ANO2 and EBNA1 (rows), in plasma samples from seven MS cases across 36 protein fragments (columns) is presented as a heatmap (D).

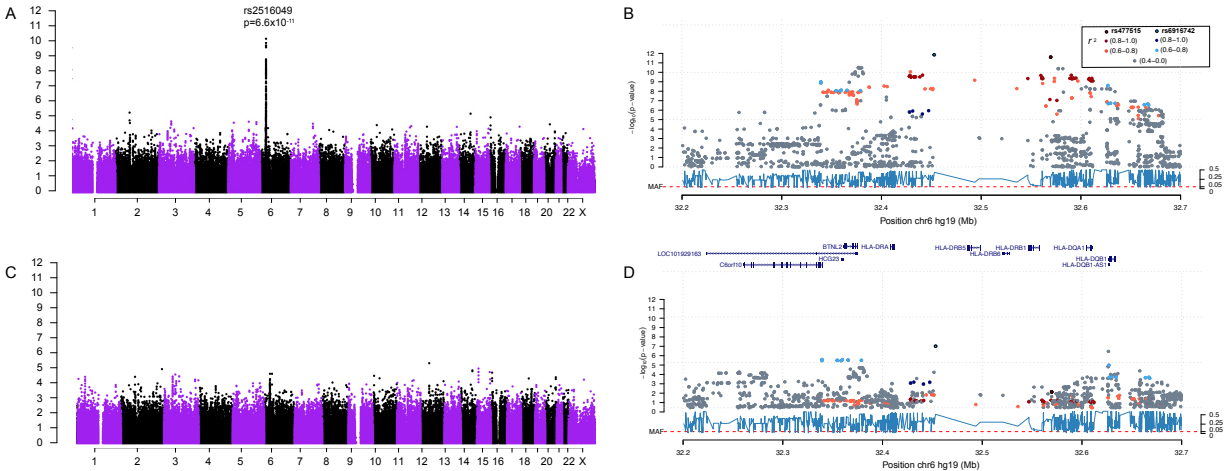


Figure S2. Genome-wide association analyses of anti-ANO2 antibody levels. A genome-wide significant signal was detected in the HLA gene region using OmniExpress genotype data (A and C). Genetic association analysis using MS replication chip genotype data resulted in the top associated SNP rs6916742 (blue) and the second top SNP rs477515 (red) displaying different patterns of linkage disequilibrium (LD; r^2) with other SNPs in the HLA gene region (B and D). Association analyses were performed with \log_{10} transformed anti-ANO2 antibody levels correcting for MS, age, sex, EBNA1-status, and principal components (A-B). When conditioning for *DRB1*04:01* and *DRB4*01:03* there was a complete loss of association using OmniExpress genotype data (C), while using MS replication chip genotype data there was complete loss of association of rs477515 and decreased association of rs6916742 (D).

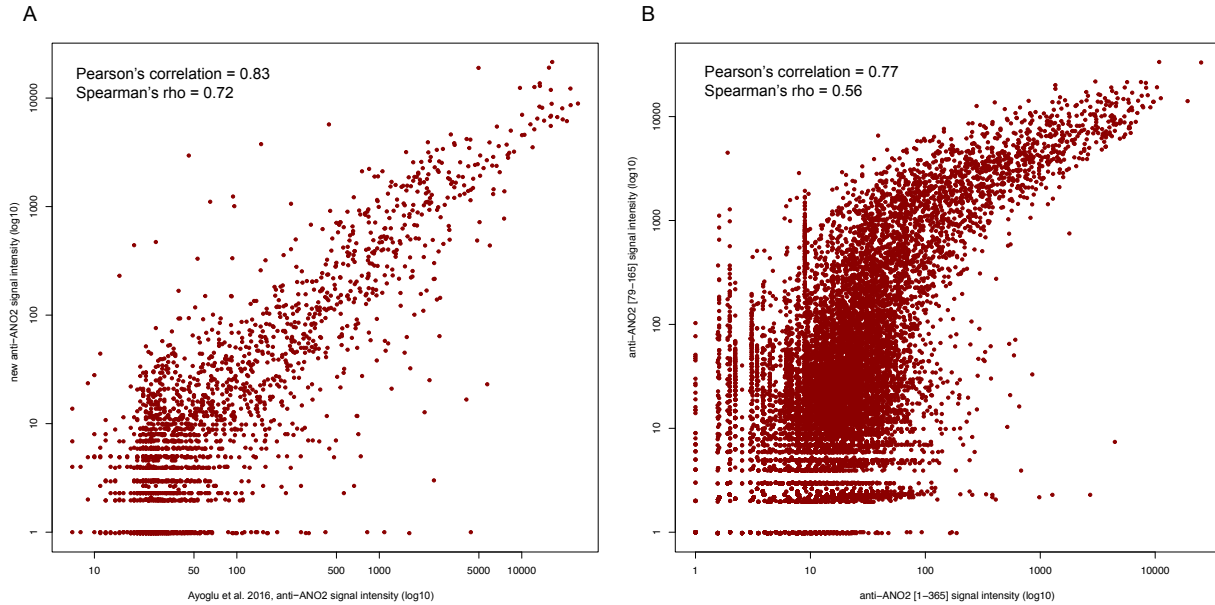


Figure S3. Correlation of anti-ANO2 intensity values between assays and representations. Log₁₀ transformed signal intensities from Aygolu et al., 2016 (x-axis) and corresponding intensities from the current study (y-axis) measured in the Initial cohort (A). Differences between methods were: Dilutions of plasma samples (1:150 versus 1:1 000) resulting in slightly different assay sensitivities, expression protocols, fusion tags (hexa histidine and albumin binding protein tag (His₆ABP) versus GST-tag), Luminex beads (MagPlex versus SeroMap), coupling chemistries of the antigens to the beads (covalent binding of primary amines versus GST-tag binding), secondary detection reagents (PE conjugated anti human IgG antibody versus combination of biotinylated anti-human IgG and streptavidin-PE conjugate) and read-out analyzers (FlexMAP 3D versus Luminex 100/200). Log₁₀ transformed signal intensities from the current study of anti-ANO2 [aa 1-365] (x-axis) and anti-ANO2 [aa 79-167] measured in the Whole cohort (y-axis) (B).

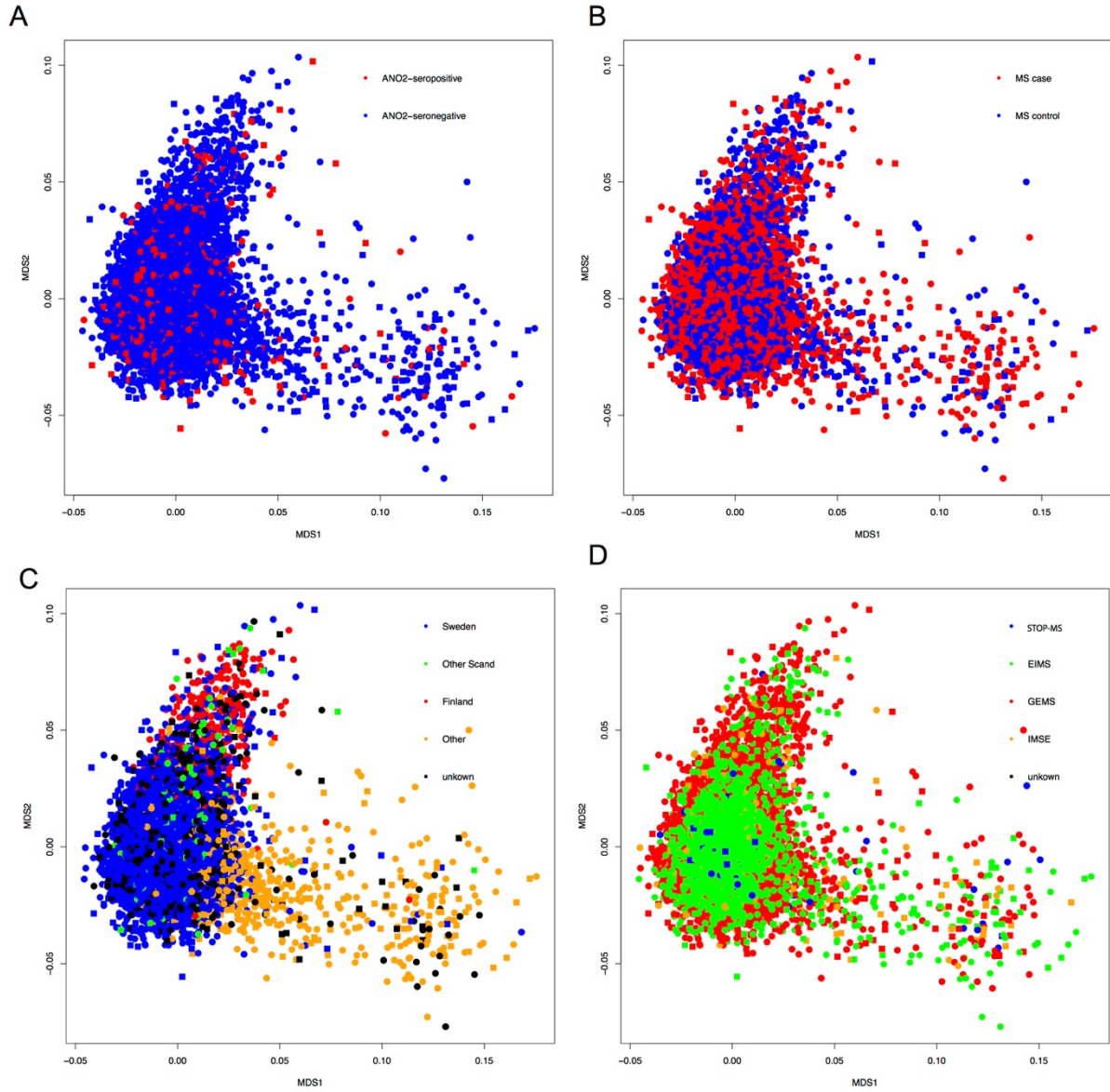


Figure S4. Multidimensional scaling plots using ancestry informative markers (AIMs). Colored for ANO2-seropositivity (A), MS-status (B), self-reported origin (C) and study cohort (D). Circles are females and squares are males.

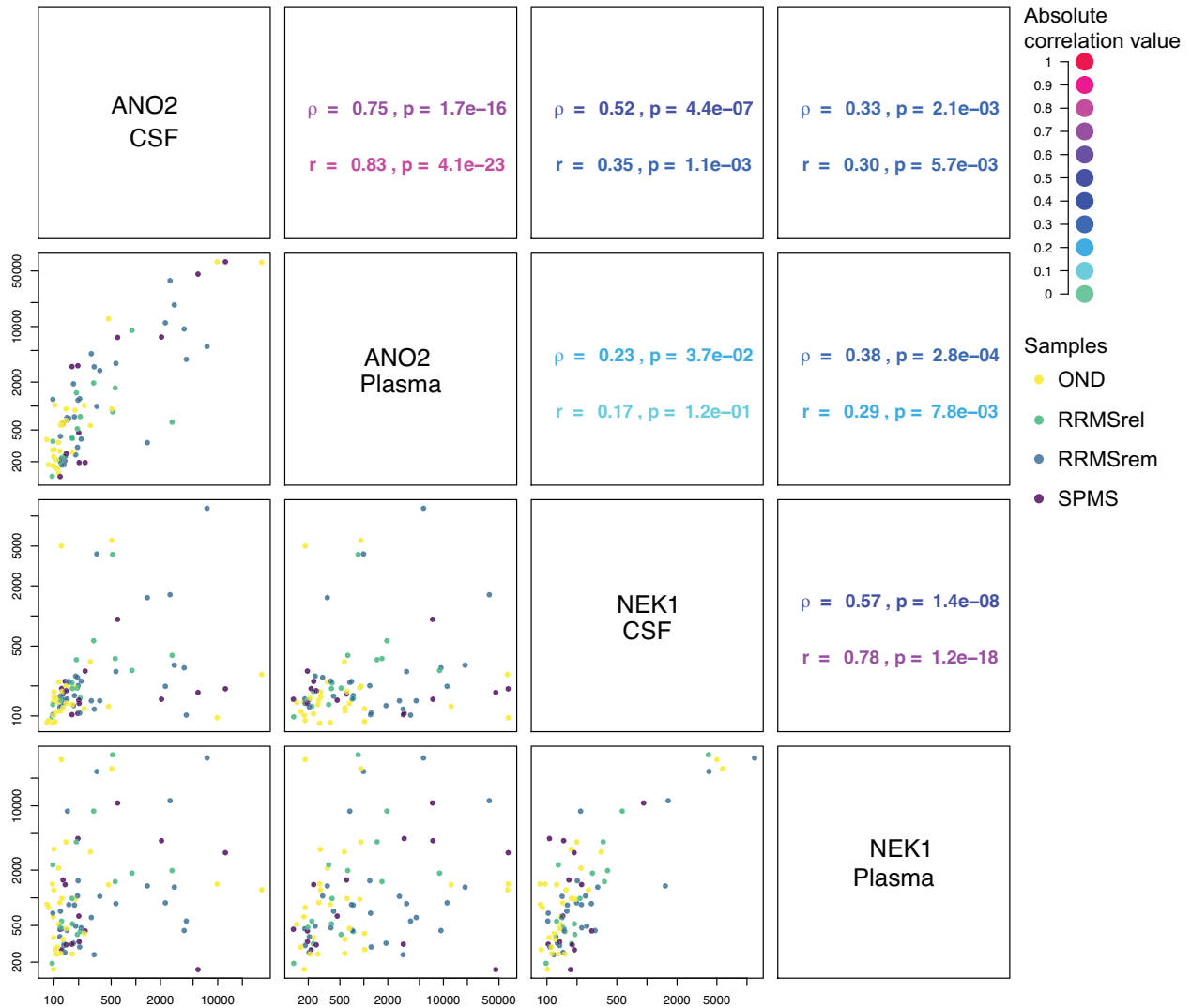


Figure S5. High correlation between ANO2 antibody reactivity in cerebrospinal fluid and plasma. In our first publication describing ANO2 as a potential autoantigen of relevance in MS (19), antibody reactivity was measured on a planar microarray in both cerebrospinal fluid (CSF) and plasma with high concordance. The same data is here presented as correlation plots including the signal intensities from the antigen representing NEK1, present on the same array, as reference. NEK1 was one of the most reactive antigens in CSF after ANO2 [aa 79-167] on the array and therefore selected as reference in the correlation analysis. A high correlation was seen between the sample types for each antigen but not between the antigens, suggesting that the ANO2 [aa 79-167] specific correlation between these two sample types is true. Signal intensities are represented by raw median fluorescent intensity (MFI). Samples were collected from patients with other neurological diseases (OND, $n = 28$), relapsing remitting MS (RRMS) in relapsing stage (RRMSrel, $n = 15$), RRMS in remitting stage (RRMSrem, $n = 28$), and secondary progressive MS (SPMS, $n = 14$). (For details regarding Materials and Methods see (19)). Correlation values were estimated with Pearson's correlation (ρ) and Spearman's rho (r).

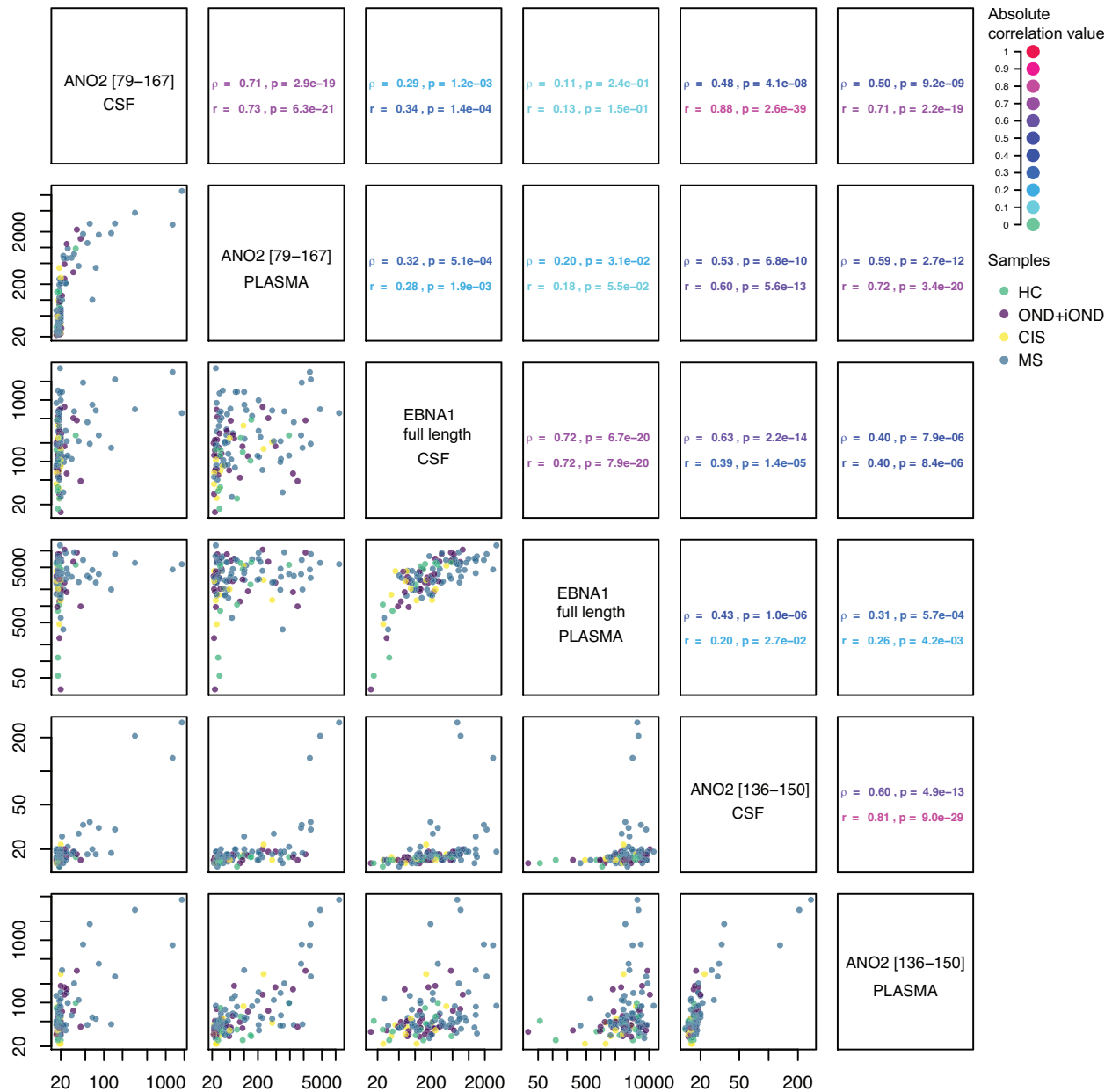


Figure S6. Correlation between ANO2 and EBNA1 antibody reactivity in cerebrospinal fluid and plasma. Additional to our first publication describing ANO2 as a potential autoantigen of relevance in MS (19), we here measured antibody reactivity towards both ANO2 and EBNA1 in a separate sample cohort on a multiplex bead array in matched CSF and plasma from 118 individuals. The methodology for generation of protein and peptide arrays and for analysis of plasma samples was applied as described in detail previously (18, 19). CSF samples were analyzed at a dilution rate of 1:50. The sample set consisted of a subset from the STOP-MS cohort (**Material S2**) including healthy controls (HC, n = 12), patients with other neurological diseases and other inflammatory neurological diseases (OND+iOND, n = 33), clinically isolated syndrome (CIS, n = 11), and MS (n = 62). Presented here are correlation plots

of the signal intensities, represented by raw median fluorescent intensity (MFI), in plasma and CSF from ANO2 [aa 79-167], EBNA1 full length, and ANO2 [aa 136-150] (peptide overlapping with ANO2 reactive epitope). In concordance to **Fig. S5**, a high correlation is detected between reactivity towards ANO2 [aa 79-167] in plasma and CSF. High antibody reactivity towards ANO2 is basically only detected in individuals with high antibody reactivity towards EBNA1. We also detect a high correlation between anti-EBNA1 antibody reactivity in plasma and CSF. Correlation values were estimated with Pearson's correlation (ρ) and Spearman's rho (r).

Table S1. Association of anti-ANO2 antibody levels with disease.

Sample cohort	Cases n	Controls n	beta	P	P (log ₁₀)	beta*	P*	P (log ₁₀)*
Initial	1 040	1 058	456	1.1x10 ⁻¹⁵	5.7x10 ⁻³⁰	428	5.0x10 ⁻¹³	6.9x10 ⁻²¹
Validation	7 603	6 170	251	1.8x10 ⁻²²	1.3x10 ⁻⁴⁶	182	7.1x10 ⁻¹²	2.3x10 ⁻²²
Whole	8 746	7 228	277	4.5x10 ⁻³²	1.8x10 ⁻⁶⁹	213	4.2x10 ⁻²⁷	3.5x10 ⁻³⁶
Pre-MS	476	478	14	0.89	1.2x10 ⁻²	-80	0.42	0.23
RA	986	689	2	0.96	0.49	-2	0.95	0.38
IIM	219	306**	11	0.52	0.46	4	0.79	0.81
SLE	349	306**	-5	0.65	0.58	-2	0.85	0.36

Association analyses were adjusted for age and sex. Analyses were also adjusted for study type for the Validation and Whole cohorts.

** Adjusted also for EBNA1-status; ** Same control set used for both IIM and SLE cohort, these controls were selected to match SLE cases*

MS=Multiple sclerosis, RA= Rheumatoid arthritis, IIM= Idiopathic inflammatory myopathy, SLE= systemic lupus erythematosus

Table S2. ANO2 seropositivity association with multiple sclerosis at different cutoffs.

Cutoff strategy	Signal intensity cutoff	ANO2+ controls n (%)	ANO2+ multiple sclerosis cases n (%)	OR (95% CI)	P	OR (95% CI)*	P*
median + 15 SD**	14 198	3 (0.041)	27 (0.31)	7.2 (2.5-30.3)	1.2x10 ⁻³	6.4 (2.2-27.5)	2.7x10 ⁻³
median + 10 SD**	9 468	17 (0.24)	81 (0.93)	3.6 (2.2-6.3)	2.0x10 ⁻⁶	3.0 (1.8-5.2)	7.4x10 ⁻⁵
median + 5 SD**	4 739	62 (0.86)	254 (2.9)	3.3 (2.5-4.4)	6.7x10 ⁻¹⁷	2.6 (2.0-3.5)	5.6x10 ⁻¹¹
median + 3 SD**	2 847	145 (2.0)	445 (5.1)	2.6 (2.1-3.1)	3.8x10 ⁻²²	2.1 (1.7-2.5)	3.5x10 ⁻¹³
median + 2 SD**	1 900	224 (3.1)	608 (7.0)	2.3 (2.0-2.7)	4.5x10 ⁻²⁵	1.8 (1.6-2.2)	8.3x10 ⁻¹⁴
median + 1 SD**	955	372 (4.5)	912 (10.4)	2.1 (1.9-2.4)	4.4x10 ⁻³¹	1.7 (1.5-2.0)	3.3x10 ⁻¹⁶
Continuous association curve (CAC)	420	566 (7.8)	1278 (14.6)	2.0 (1.8-2.2)	5.7x10 ⁻³⁸	1.6 (1.5-1.8)	3.5x10 ⁻¹⁹
mean**	208	793 (11.0)	1618 (18.5)	1.8 (1.7-2.0)	1.5x10 ⁻³⁷	1.5 (1.4-1.7)	2.7x10 ⁻¹⁸
Quartiles (top 25% vs. bottom 25%***	57	1407 (40.0)	2584 (58.0)	1.9 (1.7-2.1)	1.8x10 ⁻⁴³	1.6 (1.5-1.8)	5.1x10 ⁻²²

*Association analyses were performed in the Whole cohort and are adjusted for age, sex, and study type. * adjusted also for EBNA1-status; ** in controls; *** Removal of individuals with a signal intensity between 3 and 57 resulting in 3 518 controls and 4 456 multiple sclerosis cases being included in analysis.*

Table S3. Odds ratios for multiple sclerosis with different combinations of the risk factors

Multiple sclerosis cases (n)	Controls (n)	Risk factors	OR	SE	CI95_L	CI95_U	P
339	42	ANO2+ DRB115:01+ A02:01- EBNA1[HIGH]	26.43	0.18	18.93	37.78	2.61x10 ⁻⁷⁷
1553	401	ANO2- DRB115:01+ A02:01- EBNA1[HIGH]	12.32	0.08	10.50	14.48	2.65x10 ⁻²⁰⁶
235	58	ANO2+ DRB115:01+ A02:01+ EBNA1[HIGH]	13.19	0.16	9.71	18.18	1.41x10 ⁻⁵⁸
1256	519	ANO2- DRB115:01+ A02:01+ EBNA1[HIGH]	7.82	0.08	6.69	9.15	5.39x10 ⁻¹⁴⁶
41	15	ANO2+ DRB115:01+ A02:01- EBNA1[LOW]	9.58	0.31	5.31	18.18	4.19x10 ⁻¹³
324	287	ANO2- DRB115:01+ A02:01- EBNA1[LOW]	3.62	0.10	2.97	4.42	5.76x10 ⁻³⁷
212	87	ANO2+ DRB115:01- A02:01- EBNA1[HIGH]	8.04	0.14	6.11	10.68	2.02x10 ⁻⁴⁸
1040	812	ANO2- DRB115:01- A02:01- EBNA1[HIGH]	4.11	0.08	3.54	4.77	7.94x10 ⁻⁷⁷
25	24	ANO2+ DRB115:01+ A02:01+ EBNA1[LOW]	3.46	0.30	1.94	6.22	2.69x10 ⁻⁰⁵
350	399	ANO2- DRB115:01+ A02:01+ EBNA1[LOW]	2.86	0.10	2.37	3.45	3.04x10 ⁻²⁸
37	37	ANO2+ DRB115:01- A02:01- EBNA1[LOW]	3.38	0.24	2.10	5.45	5.39x10 ⁻⁰⁷
446	960	ANO2- DRB115:01- A02:01- EBNA1[LOW]	1.48	0.08	1.26	1.75	1.88x10 ⁻⁰⁶
108	141	ANO2+ DRB115:01- A02:01+ EBNA1[HIGH]	2.48	0.14	1.87	3.27	2.17x10 ⁻¹⁰
699	1056	ANO2- DRB115:01- A02:01+ EBNA1[HIGH]	2.09	0.08	1.80	2.44	6.37x10 ⁻²²
19	52	ANO2+ DRB115:01- A02:01+ EBNA1[LOW]	1.16	0.28	0.66	1.97	5.92x10 ⁻⁰¹
378	1208	ANO2- DRB115:01- A02:01+ EBNA1[LOW]	1	-	-	-	-

Table S4. Top SNPs ($p < 10^{-4}$) from GWAS using the OmniExpress chip

SNP	CHR	POS	A1	A2	N	eff A2	se eff A2	chi2 1df	P	raw-P (no covariates)
RS1009113	1	7143807	G	A	11929	0.066	0.016	16.2	5.75×10^{-05}	1.86×10^{-05}
RS990276	2	78542946	G	A	11904	0.061	0.014	18.5	1.70×10^{-05}	1.09×10^{-05}
RS9309532	2	78594007	A	G	11929	0.064	0.014	20.8	5.18×10^{-06}	2.65×10^{-06}
RS1006154	2	80551464	G	A	11933	0.073	0.017	17.7	2.55×10^{-05}	2.67×10^{-05}
RS2463492	2	201465718	C	A	11936	-0.047	0.012	15.5	8.22×10^{-05}	6.68×10^{-05}
RS2465665	2	201478264	A	G	11904	-0.047	0.012	15.6	7.98×10^{-05}	6.53×10^{-05}
RS12637576	3	49237334	A	G	11926	0.049	0.012	15.4	8.80×10^{-05}	1.07×10^{-04}
RS12631989	3	49273996	A	G	11908	0.048	0.012	15.2	9.80×10^{-05}	1.20×10^{-04}
RS4688454	3	64405996	A	G	11935	0.052	0.013	16.3	5.27×10^{-05}	4.36×10^{-05}
RS17354320	3	69513028	A	C	11920	0.059	0.014	18.2	1.97×10^{-05}	1.11×10^{-05}
RS9843168	3	69513198	G	A	11934	0.057	0.014	17.3	3.27×10^{-05}	1.73×10^{-05}
RS17367084	3	69513547	A	G	11933	0.058	0.014	17.7	2.63×10^{-05}	1.50×10^{-05}
RS9858836	3	86318521	G	A	11926	0.052	0.013	15.7	7.42×10^{-05}	6.34×10^{-05}
RS11926519	3	86356130	G	A	11933	0.052	0.013	15.8	6.87×10^{-05}	6.12×10^{-05}
RS9848250	3	86384224	A	C	11909	0.051	0.013	15.3	9.27×10^{-05}	8.89×10^{-05}
RS13082563	3	195057001	G	A	11924	0.068	0.017	16.2	5.56×10^{-05}	3.74×10^{-05}
RS1038591	5	22670144	G	A	11933	0.050	0.013	15.6	7.80×10^{-05}	1.58×10^{-05}
RS6860776	5	22699592	A	G	11927	0.049	0.013	15.3	9.05×10^{-05}	2.42×10^{-05}
RS6863125	5	31806258	G	A	11933	-0.064	0.015	17.8	2.44×10^{-05}	1.20×10^{-05}
RS4607382	5	116208147	G	A	11901	0.048	0.012	15.4	8.55×10^{-05}	7.40×10^{-05}
RS6859942	5	116211296	G	A	11865	0.051	0.012	18.1	2.08×10^{-05}	1.85×10^{-05}
RS1972623	5	116222219	A	G	11934	0.051	0.013	15.8	7.07×10^{-05}	6.84×10^{-05}
RS6889446	5	158901965	A	G	11924	0.060	0.014	17.4	3.00×10^{-05}	3.14×10^{-05}
RS10515797	5	158915287	G	A	11932	0.071	0.017	18.0	2.22×10^{-05}	1.44×10^{-05}
RS2735052	6	29701564	G	A	11934	-0.048	0.012	15.6	7.77×10^{-05}	1.59×10^{-05}
RS2523395	6	29702510	G	A	11933	-0.048	0.012	16.2	5.78×10^{-05}	1.14×10^{-05}
RS2394160	6	29703262	A	G	11927	-0.048	0.012	15.7	7.34×10^{-05}	1.51×10^{-05}
RS2844831	6	29706277	A	G	11927	-0.048	0.012	16.3	5.55×10^{-05}	1.08×10^{-05}
RS2743951	6	29709234	G	A	11923	-0.048	0.012	15.6	7.79×10^{-05}	1.46×10^{-05}
RS2524084	6	31241639	A	G	11934	-0.048	0.012	15.4	8.76×10^{-05}	2.64×10^{-06}
RS2523627	6	31346445	A	C	11917	0.050	0.012	16.5	4.75×10^{-05}	8.80×10^{-06}
RS2857600	6	31582287	G	A	11933	0.061	0.015	17.2	3.31×10^{-05}	7.07×10^{-07}
RS2736177	6	31586094	A	G	11934	0.059	0.015	16.1	5.87×10^{-05}	1.35×10^{-06}
RS3130071	6	31594628	T	A	11876	0.063	0.015	18.5	1.67×10^{-05}	3.62×10^{-07}
RS1046080	6	31595882	A	C	11930	0.056	0.013	19.2	1.19×10^{-05}	2.84×10^{-07}
RS2272593	6	31601344	G	A	11915	0.057	0.013	19.5	1.00×10^{-05}	2.28×10^{-07}
RS3132453	6	31604044	C	A	11931	0.083	0.019	19.0	1.28×10^{-05}	3.65×10^{-07}

RS3130050	6	31618761	A	G	11923	0.063	0.015	18.7	1.53x10 ⁻⁰⁵	2.52x10 ⁻⁰⁷
RS3130617	6	31627523	A	G	11916	0.056	0.013	18.8	1.45x10 ⁻⁰⁵	3.46x10 ⁻⁰⁷
RS3117578	6	31636031	G	A	11933	0.063	0.015	19.0	1.28x10 ⁻⁰⁵	2.17x10 ⁻⁰⁷
RS3115667	6	31643399	G	A	11931	0.056	0.013	19.3	1.14x10 ⁻⁰⁵	2.74x10 ⁻⁰⁷
RS1475865	6	31657413	G	A	11932	0.057	0.013	19.3	1.11x10 ⁻⁰⁵	2.61x10 ⁻⁰⁷
RS3117572	6	31717692	G	A	11933	0.063	0.014	20.4	6.36x10 ⁻⁰⁶	1.93x10 ⁻⁰⁷
RS2227956	6	31778272	A	G	11931	0.061	0.014	19.1	1.22x10 ⁻⁰⁵	3.54x10 ⁻⁰⁷
RS9267576	6	31812038	C	A	11931	0.070	0.015	23.0	1.63x10 ⁻⁰⁶	2.23x10 ⁻⁰⁸
RS9267577	6	31813774	G	A	11931	0.064	0.014	21.3	3.91x10 ⁻⁰⁶	7.77x10 ⁻⁰⁸
RS9267649	6	31824828	G	A	11917	0.066	0.014	22.0	2.68x10 ⁻⁰⁶	4.71x10 ⁻⁰⁸
RS9267658	6	31845985	G	A	11930	0.064	0.015	19.4	1.06x10 ⁻⁰⁵	1.60x10 ⁻⁰⁷
RS28435656	6	31880637	G	A	11923	0.054	0.013	16.0	6.39x10 ⁻⁰⁵	8.13x10 ⁻⁰⁷
RS3130683	6	31888367	A	G	11919	0.061	0.014	18.2	1.98x10 ⁻⁰⁵	1.79x10 ⁻⁰⁷
RS1048709	6	31914935	G	A	11931	0.054	0.013	16.7	4.32x10 ⁻⁰⁵	3.44x10 ⁻⁰⁷
RS3130287	6	32050544	A	G	11918	0.061	0.014	18.0	2.21x10 ⁻⁰⁵	1.99x10 ⁻⁰⁷
RS3134954	6	32071893	A	G	11935	0.059	0.014	16.8	4.12x10 ⁻⁰⁵	4.65x10 ⁻⁰⁷
RS3130342	6	32080146	C	A	11930	0.062	0.014	18.6	1.58x10 ⁻⁰⁵	1.40x10 ⁻⁰⁷
RS3130279	6	32112626	G	A	11935	0.064	0.014	20.6	5.78x10 ⁻⁰⁶	2.90x10 ⁻⁰⁸
RS3131283	6	32119898	G	A	11932	0.063	0.014	19.9	8.37x10 ⁻⁰⁶	4.56x10 ⁻⁰⁸
RS3134603	6	32126002	G	A	11931	0.068	0.015	22.2	2.50x10 ⁻⁰⁶	1.71x10 ⁻⁰⁸
RS3130283	6	32138545	C	A	11817	0.061	0.014	18.2	1.98x10 ⁻⁰⁵	1.35x10 ⁻⁰⁷
RS3134943	6	32147761	G	A	11933	0.062	0.014	19.6	9.71x10 ⁻⁰⁶	5.82x10 ⁻⁰⁸
RS1800684	6	32151994	A	T	11931	0.063	0.014	19.9	8.18x10 ⁻⁰⁶	4.30x10 ⁻⁰⁸
RS3132940	6	32161396	C	A	11928	0.066	0.014	21.5	3.48x10 ⁻⁰⁶	1.47x10 ⁻⁰⁸
RS3132946	6	32190028	G	A	11933	0.067	0.014	22.3	2.31x10 ⁻⁰⁶	8.14x10 ⁻⁰⁹
RS915894	6	32190390	A	C	11930	-0.052	0.013	16.7	4.27x10 ⁻⁰⁵	3.52x10 ⁻⁰⁸
RS2267644	6	32192560	G	A	11915	-0.114	0.028	16.8	4.18x10 ⁻⁰⁵	1.16x10 ⁻⁰⁴
RS9268199	6	32278635	A	G	11928	0.055	0.013	18.0	2.22x10 ⁻⁰⁵	3.09x10 ⁻⁰⁸
RS6910071	6	32282854	A	G	11930	-0.076	0.015	25.9	3.69x10 ⁻⁰⁷	6.85x10 ⁻⁰⁹
RS2273017	6	32337630	A	G	11934	0.052	0.012	18.7	1.57x10 ⁻⁰⁵	3.87x10 ⁻⁰⁸
RS2073044	6	32338986	G	A	11934	-0.078	0.014	29.9	4.48x10 ⁻⁰⁸	6.49x10 ⁻¹⁰
RS2076536	6	32339348	A	G	11894	0.067	0.012	30.8	2.82x10 ⁻⁰⁸	2.41x10 ⁻¹²
RS2073045	6	32339548	G	A	11927	-0.051	0.013	16.3	5.29x10 ⁻⁰⁵	4.37x10 ⁻⁰⁸
RS2050188	6	32339897	A	G	11901	0.070	0.012	32.8	1.04x10 ⁻⁰⁸	1.51x10 ⁻¹⁴
RS9268403	6	32341473	A	G	11932	-0.082	0.014	32.7	1.07x10 ⁻⁰⁸	1.47x10 ⁻¹¹
RS9268404	6	32341719	G	A	11812	-0.082	0.014	31.7	1.83x10 ⁻⁰⁸	2.95x10 ⁻¹¹
RS9268425	6	32344376	G	A	11932	-0.082	0.014	32.4	1.23x10 ⁻⁰⁸	1.68x10 ⁻¹¹
RS9268428	6	32344973	C	A	11932	-0.082	0.014	32.7	1.08x10 ⁻⁰⁸	1.46x10 ⁻¹¹
RS2894252	6	32345443	G	A	11927	-0.082	0.014	32.1	1.50x10 ⁻⁰⁸	2.11x10 ⁻¹¹
RS2395153	6	32345595	G	C	11867	-0.067	0.013	27.4	1.64x10 ⁻⁰⁷	5.75x10 ⁻¹⁰

RS8180664	6	32347490	G	A	11921	-0.082	0.014	32.5	1.22x10 ⁻⁰⁸	1.68x10 ⁻¹¹
RS9268454	6	32349711	A	G	11928	-0.082	0.014	32.6	1.12x10 ⁻⁰⁸	1.52x10 ⁻¹¹
RS9268456	6	32349946	C	A	11925	-0.082	0.014	32.5	1.17x10 ⁻⁰⁸	1.75x10 ⁻¹¹
RS9268460	6	32351283	A	G	11928	-0.057	0.012	21.0	4.70x10 ⁻⁰⁶	7.79x10 ⁻⁰⁸
RS9268461	6	32351901	C	A	11925	-0.082	0.014	32.1	1.49x10 ⁻⁰⁸	2.19x10 ⁻¹¹
RS4424066	6	32354428	A	G	11926	-0.057	0.012	21.1	4.34x10 ⁻⁰⁶	7.33x10 ⁻⁰⁸
RS9268472	6	32355605	G	A	11934	-0.056	0.012	20.9	4.90x10 ⁻⁰⁶	8.51x10 ⁻⁰⁸
RS9268474	6	32357165	A	G	11928	-0.082	0.014	32.3	1.31x10 ⁻⁰⁸	1.72x10 ⁻¹¹
RS3117098	6	32358513	A	G	11931	0.063	0.012	26.2	3.06x10 ⁻⁰⁷	2.98x10 ⁻¹²
RS3817973	6	32361111	G	A	11926	-0.057	0.012	21.2	4.23x10 ⁻⁰⁶	6.91x10 ⁻⁰⁸
RS2076529	6	32363955	A	G	11929	-0.057	0.012	21.1	4.28x10 ⁻⁰⁶	7.54x10 ⁻⁰⁸
RS3129954	6	32365580	G	A	11929	0.065	0.012	27.3	1.73x10 ⁻⁰⁷	1.43x10 ⁻¹²
RS3129955	6	32365840	G	A	11927	0.065	0.012	27.3	1.73x10 ⁻⁰⁷	1.49x10 ⁻¹²
RS2294878	6	32367795	C	A	11936	-0.070	0.012	33.6	6.81x10 ⁻⁰⁹	3.16x10 ⁻¹¹
RS3817963	6	32368087	A	G	11930	-0.081	0.014	32.1	1.48x10 ⁻⁰⁸	2.38x10 ⁻¹¹
RS2076525	6	32370616	A	G	11920	-0.082	0.014	31.9	1.59x10 ⁻⁰⁸	2.15x10 ⁻¹¹
RS2076524	6	32370684	A	G	11934	-0.082	0.014	32.6	1.11x10 ⁻⁰⁸	1.51x10 ⁻¹¹
RS2076523	6	32370835	A	G	11931	-0.082	0.013	40.5	1.99x10 ⁻¹⁰	5.71x10 ⁻¹³
RS3793127	6	32371915	G	A	11934	-0.082	0.015	29.5	5.48x10 ⁻⁰⁸	5.78x10 ⁻¹⁰
RS3806157	6	32373801	A	C	11853	-0.083	0.013	41.4	1.25x10 ⁻¹⁰	3.56x10 ⁻¹³
RS9268493	6	32375330	G	A	11928	-0.075	0.014	28.4	1.00x10 ⁻⁰⁷	1.34x10 ⁻¹⁰
RS9268494	6	32375352	A	C	11933	-0.074	0.014	28.3	1.03x10 ⁻⁰⁷	1.59x10 ⁻¹⁰
RS6926737	6	32375745	G	A	11936	-0.073	0.012	36.5	1.51x10 ⁻⁰⁹	6.52x10 ⁻¹³
RS3763309	6	32375973	C	A	11930	-0.082	0.015	29.4	5.94x10 ⁻⁰⁸	6.07x10 ⁻¹⁰
RS3763311	6	32376176	G	A	11930	-0.075	0.014	27.8	1.35x10 ⁻⁰⁷	2.69x10 ⁻¹⁰
RS3763312	6	32376348	G	A	11816	-0.081	0.015	28.5	9.50x10 ⁻⁰⁸	1.37x10 ⁻⁰⁹
RS3763316	6	32376746	G	A	11932	-0.081	0.014	31.8	1.71x10 ⁻⁰⁸	2.53x10 ⁻¹¹
RS3763317	6	32376788	G	A	11929	-0.068	0.012	31.0	2.55x10 ⁻⁰⁸	1.02x10 ⁻¹⁰
RS9268503	6	32377061	G	A	11928	-0.071	0.012	34.9	3.43x10 ⁻⁰⁹	2.01x10 ⁻¹²
RS5007265	6	32378866	A	C	11927	-0.072	0.012	36.0	2.02x10 ⁻⁰⁹	9.56x10 ⁻¹³
RS5007263	6	32378982	A	G	11928	-0.072	0.012	35.6	2.39x10 ⁻⁰⁹	1.20x10 ⁻¹²
RS5007259	6	32379101	A	G	11936	-0.072	0.012	36.1	1.85x10 ⁻⁰⁹	8.71x10 ⁻¹³
RS9268516	6	32379489	G	A	11927	-0.081	0.014	32.2	1.42x10 ⁻⁰⁸	1.88x10 ⁻¹¹
RS6932810	6	32380190	G	A	11921	-0.072	0.012	35.3	2.76x10 ⁻⁰⁹	1.58x10 ⁻¹²
RS6932542	6	32380262	A	G	11932	-0.072	0.012	36.2	1.78x10 ⁻⁰⁹	8.34x10 ⁻¹³
RS9268541	6	32384527	A	G	11922	0.118	0.029	16.8	4.23x10 ⁻⁰⁵	4.02x10 ⁻⁰⁶
RS2395163	6	32387809	A	G	11931	-0.084	0.015	30.9	2.76x10 ⁻⁰⁸	1.94x10 ⁻¹⁰
RS2395175	6	32405026	G	A	11925	-0.075	0.016	22.5	2.13x10 ⁻⁰⁶	3.03x10 ⁻⁰⁸
RS3129882	6	32409530	A	G	11927	0.047	0.012	15.5	8.07x10 ⁻⁰⁵	2.69x10 ⁻⁰⁸
RS9268658	6	32410716	G	A	11934	-0.052	0.013	16.9	4.02x10 ⁻⁰⁵	2.03x10 ⁻⁰⁶

RS2239804	6	32411523	A	G	11927	-0.052	0.013	16.6	4.72x10 ⁻⁰⁵	2.38x10 ⁻⁰⁶
RS2239803	6	32411833	G	A	11920	-0.052	0.013	17.2	3.30x10 ⁻⁰⁵	1.31x10 ⁻⁰⁶
RS9268831	6	32427748	G	A	11932	-0.050	0.012	16.6	4.71x10 ⁻⁰⁵	4.09x10 ⁻⁰⁶
RS6923504	6	32428186	C	G	11928	0.050	0.012	16.5	4.83x10 ⁻⁰⁵	7.70x10 ⁻⁰⁹
RS6903608	6	32428285	A	G	11933	0.051	0.012	16.7	4.45x10 ⁻⁰⁵	6.57x10 ⁻⁰⁹
RS9268853	6	32429643	A	G	11914	-0.082	0.014	34.5	4.16x10 ⁻⁰⁹	1.21x10 ⁻¹²
RS9268877	6	32431147	G	A	11927	0.051	0.012	17.5	2.90x10 ⁻⁰⁵	6.56x10 ⁻⁰⁹
RS9268880	6	32431358	C	A	11905	0.053	0.012	18.3	1.91x10 ⁻⁰⁵	2.08x10 ⁻⁰⁹
RS2395185	6	32433167	C	A	11926	-0.081	0.014	33.9	5.88x10 ⁻⁰⁹	1.90x10 ⁻¹²
RS9268979	6	32435044	G	A	11825	0.050	0.012	17.2	3.45x10 ⁻⁰⁵	8.70x10 ⁻⁰⁹
RS9368726	6	32438542	A	G	11882	-0.080	0.014	33.5	6.97x10 ⁻⁰⁹	2.62x10 ⁻¹²
RS9405108	6	32438648	G	A	11928	-0.080	0.014	33.5	6.96x10 ⁻⁰⁹	2.22x10 ⁻¹²
RS9286790	6	32439828	G	A	11933	-0.081	0.014	34.2	5.07x10 ⁻⁰⁹	1.61x10 ⁻¹²
RS1964995	6	32449411	A	G	11923	-0.065	0.012	26.9	2.13x10 ⁻⁰⁷	2.12x10 ⁻¹⁰
RS28366298	6	32560859	A	C	11885	-0.081	0.014	33.5	7.04x10 ⁻⁰⁹	2.29x10 ⁻¹²
RS35265698	6	32561334	C	G	11795	-0.095	0.016	34.0	5.61x10 ⁻⁰⁹	3.02x10 ⁻¹¹
RS477515	6	32569691	G	A	11871	-0.090	0.014	40.7	1.82x10 ⁻¹⁰	2.44x10 ⁻¹⁴
RS2516049	6	32570400	A	G	11920	-0.092	0.014	42.6	6.59x10 ⁻¹¹	7.30x10 ⁻¹⁵
RS602457	6	32573562	A	G	11935	-0.093	0.016	33.3	8.01x10 ⁻⁰⁹	2.51x10 ⁻¹¹
RS660895	6	32577380	A	G	11936	-0.093	0.015	40.1	2.44x10 ⁻¹⁰	5.26x10 ⁻¹³
RS532098	6	32578052	G	A	11928	-0.052	0.012	18.1	2.13x10 ⁻⁰⁵	1.10x10 ⁻⁰⁷
RS9271488	6	32589000	C	A	11908	-0.078	0.014	31.3	2.24x10 ⁻⁰⁸	9.03x10 ⁻¹²
RS9271588	6	32590953	A	G	11898	-0.058	0.012	22.5	2.07x10 ⁻⁰⁶	4.74x10 ⁻⁰⁹
RS17843604	6	32620283	G	A	11873	-0.059	0.012	23.3	1.36x10 ⁻⁰⁶	3.56x10 ⁻¹⁰
RS9273349	6	32625869	A	G	11933	-0.070	0.012	32.5	1.16x10 ⁻⁰⁸	4.11x10 ⁻¹³
RS6928482	6	32626249	A	G	11886	-0.063	0.013	25.1	5.51x10 ⁻⁰⁷	1.17x10 ⁻⁰⁸
RS1063355	6	32627714	A	C	11924	-0.070	0.012	33.1	8.95x10 ⁻⁰⁹	2.75x10 ⁻¹³
RS9273448	6	32627747	G	A	11932	0.062	0.012	24.6	7.16x10 ⁻⁰⁷	1.03x10 ⁻¹⁰
RS2647025	6	32635949	G	A	11927	-0.069	0.014	25.0	5.75x10 ⁻⁰⁷	2.35x10 ⁻⁰⁹
RS9274741	6	32637994	A	G	11830	-0.051	0.012	17.0	3.66x10 ⁻⁰⁵	3.34x10 ⁻⁰⁶
RS9275141	6	32651117	A	C	11897	-0.063	0.013	25.6	4.28x10 ⁻⁰⁷	1.39x10 ⁻⁰⁸
RS2856695	6	32651894	A	G	11931	-0.064	0.013	26.1	3.19x10 ⁻⁰⁷	1.04x10 ⁻⁰⁸
RS3021058	6	32652359	A	C	11922	-0.064	0.013	26.0	3.42x10 ⁻⁰⁷	1.06x10 ⁻⁰⁸
RS4947342	6	32653070	G	A	11906	-0.083	0.014	33.1	8.85x10 ⁻⁰⁹	2.86x10 ⁻¹¹
RS2856692	6	32653385	A	C	11886	-0.082	0.014	32.1	1.43x10 ⁻⁰⁸	4.98x10 ⁻¹¹
RS4642516	6	32657543	C	A	11929	-0.064	0.013	26.2	3.09x10 ⁻⁰⁷	9.87x10 ⁻⁰⁹
RS7774434	6	32657578	A	G	11934	-0.052	0.013	16.9	3.91x10 ⁻⁰⁵	9.91x10 ⁻⁰⁷
RS2858324	6	32660375	A	G	11918	-0.058	0.012	23.7	1.14x10 ⁻⁰⁶	3.54x10 ⁻⁰⁸
RS5000634	6	32663564	A	G	11906	-0.058	0.013	20.1	7.20x10 ⁻⁰⁶	2.08x10 ⁻⁰⁶
RS6457617	6	32663851	G	A	11921	-0.050	0.012	17.3	3.11x10 ⁻⁰⁵	6.73x10 ⁻⁰⁶

RS6457622	6	32664163	A	C	11923	-0.058	0.013	20.0	7.81x10 ⁻⁰⁶	2.09x10 ⁻⁰⁶
RS2647012	6	32664458	A	G	11932	-0.057	0.012	23.0	1.60x10 ⁻⁰⁶	4.86x10 ⁻⁰⁸
RS2647003	6	32664880	A	C	11931	-0.057	0.012	23.0	1.61x10 ⁻⁰⁶	5.06x10 ⁻⁰⁸
RS9275312	6	32665728	A	G	11923	-0.074	0.016	22.1	2.58x10 ⁻⁰⁶	1.32x10 ⁻⁰⁷
RS2856725	6	32666738	G	A	11930	-0.057	0.012	23.0	1.65x10 ⁻⁰⁶	4.98x10 ⁻⁰⁸
RS9275328	6	32666822	G	A	11929	-0.072	0.016	21.1	4.27x10 ⁻⁰⁶	2.45x10 ⁻⁰⁷
RS9275330	6	32666875	A	G	11914	-0.071	0.016	20.6	5.68x10 ⁻⁰⁶	3.18x10 ⁻⁰⁷
RS9275333	6	32666968	A	G	11931	-0.073	0.016	21.3	4.02x10 ⁻⁰⁶	2.23x10 ⁻⁰⁷
RS3135006	6	32667119	G	A	11862	0.061	0.012	23.8	1.05x10 ⁻⁰⁶	1.62x10 ⁻¹⁰
RS9275371	6	32668296	A	G	11919	-0.052	0.013	15.2	9.81x10 ⁻⁰⁵	8.79x10 ⁻⁰⁶
RS1612904	6	32669018	A	C	11908	0.048	0.012	16.1	6.15x10 ⁻⁰⁵	4.25x10 ⁻⁰⁶
RS2856717	6	32670308	A	G	11933	-0.058	0.012	23.5	1.22x10 ⁻⁰⁶	3.46x10 ⁻⁰⁸
RS2858305	6	32670464	C	A	11932	-0.058	0.012	23.2	1.48x10 ⁻⁰⁶	4.51x10 ⁻⁰⁸
RS4947344	6	32677846	G	A	11903	0.056	0.012	21.3	3.93x10 ⁻⁰⁶	1.34x10 ⁻⁰⁹
RS7454108	6	32681483	A	G	11923	-0.080	0.018	19.6	9.52x10 ⁻⁰⁶	7.75x10 ⁻⁰⁷
RS3957146	6	32681530	A	G	11891	-0.081	0.018	19.7	9.13x10 ⁻⁰⁶	7.77x10 ⁻⁰⁷
RS9275596	6	32681631	A	G	11923	0.047	0.012	15.7	7.36x10 ⁻⁰⁵	5.11x10 ⁻⁰⁶
RS3998159	6	32682019	A	C	11921	-0.079	0.018	19.0	1.29x10 ⁻⁰⁵	1.05x10 ⁻⁰⁶
RS3957148	6	32682137	A	G	11925	-0.081	0.018	20.1	7.53x10 ⁻⁰⁶	7.20x10 ⁻⁰⁷
RS13192583	6	43834027	G	A	11936	-0.097	0.024	16.3	5.54x10 ⁻⁰⁵	2.63x10 ⁻⁰⁵
RS9692521	7	124956491	G	A	11905	0.056	0.014	16.7	4.32x10 ⁻⁰⁵	7.15x10 ⁻⁰⁵
RS6973477	7	124958806	A	C	11912	0.055	0.014	16.2	5.61x10 ⁻⁰⁵	7.45x10 ⁻⁰⁵
RS7795867	7	124977736	A	G	11926	0.057	0.014	17.5	2.82x10 ⁻⁰⁵	4.03x10 ⁻⁰⁵
RS4419802	8	57216066	G	A	11935	-0.052	0.013	15.7	7.39x10 ⁻⁰⁵	1.68x10 ⁻⁰⁵
RS6473170	8	80502285	G	A	11885	0.050	0.013	15.2	9.48x10 ⁻⁰⁵	1.76x10 ⁻⁰⁴
RS10508855	10	37070799	G	A	11907	0.132	0.032	17.1	3.50x10 ⁻⁰⁵	1.51x10 ⁻⁰⁵
RS12358208	10	123470963	G	A	11916	0.074	0.019	15.9	6.77x10 ⁻⁰⁵	7.64x10 ⁻⁰⁵
RS638051	11	68141414	A	G	11905	0.048	0.012	15.3	9.35x10 ⁻⁰⁵	1.58x10 ⁻⁰⁴
RS3740925	11	87847018	A	G	11913	-0.081	0.020	16.4	5.02x10 ⁻⁰⁵	6.57x10 ⁻⁰⁵
RS1943509	11	95319115	G	A	11904	0.058	0.014	16.9	4.03x10 ⁻⁰⁵	1.95x10 ⁻⁰⁴
RS12582594	12	48810729	G	A	11929	-0.062	0.015	16.7	4.46x10 ⁻⁰⁵	2.89x10 ⁻⁰⁵
RS11616341	13	101721029	A	G	11931	-0.054	0.013	16.6	4.54x10 ⁻⁰⁵	4.72x10 ⁻⁰⁵
RS6574723	14	83306515	G	A	11927	0.064	0.014	20.5	6.09x10 ⁻⁰⁶	4.28x10 ⁻⁰⁵
RS1024307	14	83308389	G	A	11918	0.064	0.014	20.5	6.09x10 ⁻⁰⁶	4.26x10 ⁻⁰⁵
RS2046362	15	30936285	G	A	11880	0.046	0.012	15.4	8.89x10 ⁻⁰⁵	5.13x10 ⁻⁰⁵
RS1437773	15	96997098	A	G	11920	-0.052	0.013	16.1	5.98x10 ⁻⁰⁵	8.29x10 ⁻⁰⁵
RS10500329	16	5894782	G	A	11900	0.054	0.012	19.4	1.07x10 ⁻⁰⁵	8.51x10 ⁻⁰⁶
RS6500728	16	5900889	G	A	11932	0.051	0.013	15.8	7.00x10 ⁻⁰⁵	1.02x10 ⁻⁰⁴
RS2343339	16	5919272	G	A	11932	0.051	0.012	17.0	3.68x10 ⁻⁰⁵	3.32x10 ⁻⁰⁵
RS11150737	17	78641290	A	G	11919	-0.053	0.013	16.7	4.45x10 ⁻⁰⁵	4.58x10 ⁻⁰⁵

RS13111	20	30922399	G	A	11901	-0.080	0.019	17.4	3.10×10^{-05}	1.28×10^{-05}
RS846215	20	59199927	G	A	11933	0.056	0.014	15.3	9.22×10^{-05}	5.43×10^{-05}
RS525126	23	90557537	A	C	11903	-0.043	0.011	16.0	6.39×10^{-05}	1.16×10^{-04}

Table S5. HLA alleles associated with anti-ANO2 antibody levels

HLA allele	ALL						CASES			CONTROLS		
	Allele frequency (%)	OR (95%CI)	OR P	beta *	P*	P (log ₁₀)	beta *	P*	P (log ₁₀)	beta *	P*	P (log ₁₀)
<i>B*15:01-DRB4*01:03-DRB1*04:[01/04]-DQA1*03:[01/02]-DQB1*03:02</i>												
<i>B*15:01</i>	20	0.8 (0.7-0.9)	2.2x10 ⁻³	-82	1.1x10 ⁻²	6.0x10 ⁻³	-153	5.4x10 ⁻³	3.7x10 ⁻³	-5	0.86	0.52
<i>DRB4*01:03</i>	38	0.7 (0.6-0.8)	5.2x10 ⁻⁹	-127	1.9x10 ⁻⁶	4.0x10 ⁻¹²	-165	3.3x10 ⁻⁴	5.3x10 ⁻⁶	-90	2.3x10 ⁻⁴	5.1x10 ⁻⁵
<i>DRB1*04:01</i>	19	0.6 (0.5-0.7)	9.7x10 ⁻¹¹	-129	9.0x10 ⁻⁵	1.7x10 ⁻¹¹	-190	1.2x10 ⁻³	4.6x10 ⁻⁶	-79	6.7x10 ⁻³	5.5x10 ⁻⁵
<i>DRB1*04:04</i>	9	0.8 (0.6-1.0)	4.3x10 ⁻²	-102	2.6x10 ⁻²	8.1x10 ⁻³	-107	0.16	5.1x10 ⁻²	-94	3.0x10 ⁻²	3.7x10 ⁻²
<i>DQA1*03:01</i>	27	0.7 (0.6-0.8)	5.3x10 ⁻⁶	-111	1.4x10 ⁻⁴	4.9x10 ⁻⁶	-158	1.6x10 ⁻³	5.0x10 ⁻⁴	-65	1.5x10 ⁻²	1.0x10 ⁻²
<i>DQA1*03:02</i>	8	0.6 (0.4-0.7)	2.0x10 ⁻⁵	-94	4.9x10 ⁻²	4.1x10 ⁻⁶	-119	0.20	3.3x10 ⁻³	-81	3.9x10 ⁻²	1.1x10 ⁻²
<i>DQB1*03:02</i>	25	0.8 (0.7-0.9)	5.7x10 ⁻⁵	-123	4.2x10 ⁻⁵	7.2x10 ⁻⁶	-177	5.7x10 ⁻⁴	2.6x10 ⁻⁴	-67	1.6x10 ⁻²	1.3x10 ⁻²
<i>A*32:01-DRB3*02:02-DRB1*12:01-DQA1*05:05</i>												
<i>A*32:01</i>	6	1.2 (0.9-1.4)	0.15	80	0.14	5.1x10 ⁻³	109	0.23	0.12	46	0.36	8.8x10 ⁻³
<i>DRB3*02:02</i>	22	1.2 (1.0-1.3)	1.8x10 ⁻²	105	9.1x10 ⁻⁴	3.0x10 ⁻³	178	1.4x10 ⁻³	8.5x10 ⁻³	42	0.14	1.2x10 ⁻³
<i>DRB1*12:01</i>	3	1.5 (1.2-1.9)	2.2x10 ⁻³	314	1.9x10 ⁻⁵	4.6x10 ⁻⁵	599	3.8x10 ⁻⁵	1.6x10 ⁻³	148	1.3x10 ⁻²	6.0x10 ⁻⁵
<i>DQA1*05:05**</i>	12	1.2 (1.0-1.4)	1.4x10 ⁻²	166	2.8x10 ⁻⁵	4.1x10 ⁻²	320	4.0x10 ⁻⁶	3.9x10 ⁻²	22	0.54	8.9x10 ⁻²
<i>B*07:02-DRB5*01:01-DRB1*15:01-DQA1*01:02-DQB*06:02</i>												
<i>B*07:02</i>	34	1.2 (1.0-1.3)	6.6x10 ⁻³	20	0.47	1.2x10 ⁻⁴	29	0.52	2.9x10 ⁻²	12	0.65	0.12
<i>DRB5*01:01</i>	45	1.3 (1.1-1.4)	5.4x10 ⁻⁵	-4	0.87	7.7x10 ⁻⁹	1	0.98	6.7x10 ⁻³	-14	0.60	0.32
<i>DRB1*15:01</i>	45	1.3 (1.1-1.4)	7.8x10 ⁻⁵	-6	0.82	2.0x10 ⁻⁸	-2	0.97	9.7x10 ⁻³	-14	0.60	0.36
<i>DQA1*01:02</i>	52	1.2 (1.1-1.4)	1.3x10 ⁻⁴	9	0.74	1.9x10 ⁻⁸	22	0.64	6.8x10 ⁻³	-7	0.77	9.9x10 ⁻²
<i>DQB1*06:02</i>	44	1.3 (1.1-1.4)	2.1x10 ⁻⁵	-1	0.96	3.4x10 ⁻⁸	-1	0.99	1.6x10 ⁻²	-6	0.82	0.31
<i>Other</i>												
<i>DQB1*06:09</i>	1	1.8 (1.2-2.5)	3.4x10 ⁻³	382	4.1x10 ⁻⁴	7.8x10 ⁻⁴	426	9.9x10 ⁻³	9.1x10 ⁻³	287	1.4x10 ⁻²	0.14

Note: Alleles included are associated at significance level $\alpha=0.01$ in all individuals ($n = 13\ 160$) with \log_{10} transformed anti-ANO2 signal intensities. All results were based on carrier association adjusted for MS (in all), age, study type, EBNA1-status, sex, and PCA1-5.

*not \log_{10} transformed, ** included in the table due to its presence on the associated haplotype

HLA haplotype references: (28-31) and <http://www.allelefrequencies.net>

Table S6. ANO2 [aa 1-365] autoantibody reactivity association with disease.

Cohort	Controls N	Cases N	beta	p	p (log ₁₀)	beta*	p*	P (log ₁₀)*
Initial	1 058	1 040	133	4.5x10 ⁻⁹	1.0x10 ⁻¹⁷	127	6.8x10 ⁻⁸	5.5x10 ⁻¹²
Validation	6 170	7 603	37	4.0x10 ⁻⁵	6.1x10 ⁻⁴	23	1.4x10 ⁻²	1.9x10 ⁻¹²
Whole	7 228	8 746	49	4.4x10 ⁻⁹	0.94	36	3.3x10 ⁻⁵	4.6x10 ⁻⁵
Pre-MS	478	476	-15	0.45	2.1x10 ⁻²	-31	0.12	0.28
RA	986	689	-22	0.21	0.41	-22	0.19	0.48

Association analyses are adjusted for age and sex. Analyses were also adjusted for study type for the Validation and Whole cohorts. *Adjusted also for EBNA1-status.

MS=Multiple sclerosis, RA= Rheumatoid arthritis.

Table S7. Demographic data of the Initial, Validation, and Whole cohorts.

Sample cohort	No. of Subjects	Female%	Median age, yrs	Range, yrs
Initial				
RRMS*	924	75	36	16-71
SPMS†	59	61	48	22-66
PPMS†	29	59	54	36-76
PRMS/RPMS†	7	43	45	33-55
<i>COURSE NA</i>	8	75	47	27-65
MS	1 040	74	37	16-76
Control	1 058	76	40	18-70
Total	2 098			
Validation				
RRMS*	4 594	74	42 (1 NA)	13-88
SPMS†	1 724	71	59	19-87
PPMS†	515	56	61.0	20-86
PRMS/RPMS†	127	69	51	20-84
<i>COURSE NA</i>	634	70	58	17-87
MS	7 604	72	48 (1 NA)	13-88
Control	6 170	75	49	16-89
Total	13 774			
Whole				
RRMS*	5 589	74	41 (1 NA)	13-88
SPMS†	1 804	71	58	19-87
PPMS†	549	56	61	20-86
PRMS/RPMS†	134	67	51	20-84
<i>COURSE NA</i>	642	74	58	17-87
MS	8 746	72	47 (1 NA)	13-88
Control	7 228	75	48	16-89
Total	15 974			

PPMS, primary progressive MS; PRMS, progressive relapsing MS; RPMS, relapsing progressive MS; RRMS, relapsing remitting MS; SPMS, secondary progressive MS.

**The CIS-conv and RRMS groups are categorized as “relapsing-remitting MS.”*

†The SPMS, PPMS, RPMS and PRMS groups are categorized as “progressive MS.”

References

1. Olafsson S, *et al.* (2017) Fourteen sequence variants that associate with multiple sclerosis discovered by meta-analysis informed by genetic correlations. *NPJ Genom Med* 2:24.
2. International Multiple Sclerosis Genetics Consortium P, N., Baranzini, S.E., Santaniello, A., Shoostari, P., Cotsapas, C., Wong, G., Beecham, A.H., James, T., Replogle, J., *et al.* (2017) The Multiple Sclerosis Genomic Map: Role of peripheral immune cells and resident microglia in susceptibility. *bioRxiv* <https://doi.org/10.1101/143933>.
3. Patterson N, Price AL, & Reich D (2006) Population structure and eigenanalysis. *PLoS Genet* 2(12):e190.
4. Purcell S, *et al.* (2007) PLINK: a tool set for whole-genome association and population-based linkage analyses. *Am J Hum Genet* 81(3):559-575.
5. Aulchenko YS, Ripke S, Isaacs A, & van Duijn CM (2007) GenABEL: an R library for genome-wide association analysis. *Bioinformatics* 23(10):1294-1296.
6. Rönnegård L, Shen X, & Alam M (2010) hglm: A package for fitting hierarchical generalized linear models. *The R Journal* 2:20-28.
7. Kierczak M, *et al.* (2015) cgmisc: enhanced genome-wide association analyses and visualization. *Bioinformatics* 31(23):3830-3831.
8. Barsh GS, Copenhaver GP, Gibson G, & Williams SM (2012) Guidelines for genome-wide association studies. *PLoS Genet* 8(7):e1002812.
9. Patsopoulos N (2016) PgmNr 4: 200 loci complete the genetic puzzle of multiple sclerosis. in *the American Society of Human Genetics 2016 Annual Meeting* (Vancouver, B.C., Canada.).
10. Dilthey A, *et al.* (2013) Multi-population classical HLA type imputation. *PLoS Comput Biol* 9(2):e1002877.
11. Jia X, *et al.* (2013) Imputing amino acid polymorphisms in human leukocyte antigens. *PLoS One* 8(6):e64683.
12. Hedstrom AK, Baarnhielm M, Olsson T, & Alfredsson L (2009) Tobacco smoking, but not Swedish snuff use, increases the risk of multiple sclerosis. *Neurology* 73(9):696-701.
13. Hedstrom AK, Akerstedt T, Hillert J, Olsson T, & Alfredsson L (2011) Shift work at young age is associated with increased risk for multiple sclerosis. *Ann Neurol* 70(5):733-741.
14. Holmen C, *et al.* (2011) A Swedish national post-marketing surveillance study of natalizumab treatment in multiple sclerosis. *Mult Scler* 17(6):708-719.
15. Khademi M, *et al.* (2011) Cerebrospinal fluid CXCL13 in multiple sclerosis: a suggestive prognostic marker for the disease course. *Mult Scler* 17(3):335-343.
16. McDonald WI, *et al.* (2001) Recommended diagnostic criteria for multiple sclerosis: guidelines from the International Panel on the diagnosis of multiple sclerosis. *Ann Neurol* 50(1):121-127.
17. Polman CH, *et al.* (2011) Diagnostic criteria for multiple sclerosis: 2010 revisions to the McDonald criteria. *Ann Neurol* 69(2):292-302.
18. Ayoglu B, *et al.* (2016) Anoctamin 2 identified as an autoimmune target in multiple sclerosis. *Proceedings of the National Academy of Sciences of the United States of America* 113(8):2188-2193.
19. Ayoglu B, *et al.* (2013) Autoantibody profiling in multiple sclerosis using arrays of human protein fragments. *Mol Cell Proteomics* 12(9):2657-2672.

20. Stolt P, *et al.* (2003) Quantification of the influence of cigarette smoking on rheumatoid arthritis: results from a population based case-control study, using incident cases. *Ann Rheum Dis* 62(9):835-841.
21. Haggmark A, *et al.* (2015) Proteomic profiling reveals autoimmune targets in sarcoidosis. *Am J Respir Crit Care Med* 191(5):574-583.
22. Idborg H, *et al.* (2018) TNF-alpha and plasma albumin as biomarkers of disease activity in systemic lupus erythematosus. *Lupus Sci Med* 5(1):e000260.
23. Waterboer T, *et al.* (2005) Multiplex human papillomavirus serology based on in situ-purified glutathione s-transferase fusion proteins. *Clin Chem* 51(10):1845-1853.
24. Sehr P, Zumbach K, & Pawlita M (2001) A generic capture ELISA for recombinant proteins fused to glutathione S-transferase: validation for HPV serology. *J Immunol Methods* 253(1-2):153-162.
25. Sundqvist E, *et al.* (2012) Epstein-Barr virus and multiple sclerosis: interaction with HLA. *Genes Immun* 13(1):14-20.
26. Team RC (2014) R: A language and environment for statistical computing. *R Foundation for Statistical Computing, Vienna, Austria.*
27. Kallberg H, Ahlbom A, & Alfredsson L (2006) Calculating measures of biological interaction using R. *Eur J Epidemiol* 21(8):571-573.
28. Farh KK, *et al.* (2015) Genetic and epigenetic fine mapping of causal autoimmune disease variants. *Nature* 518(7539):337-343.
29. Patsopoulos NA, *et al.* (2013) Fine-mapping the genetic association of the major histocompatibility complex in multiple sclerosis: HLA and non-HLA effects. *PLoS Genet* 9(11):e1003926.
30. Erlich HA, *et al.* (2013) Next generation sequencing reveals the association of DRB3*02:02 with type 1 diabetes. *Diabetes* 62(7):2618-2622.
31. Maiers M, Gragert L, & Klitz W (2007) High-resolution HLA alleles and haplotypes in the United States population. *Hum Immunol* 68(9):779-788.